PNAS
www.pnas.org

Supplementary Information for

Modeling SHH-driven medulloblastoma with patient iPS cell-derived neural stem cells

Evelyn Susanto, Ana Marin Navarro, Leilei Zhou, Anders Sundström, Niek van Bree, Marina Stantic, Mohsen Moslem, Jignesh Tailor, Jonne Rietdijk, Veronica Zubillaga, Jens-Martin Hübner, Holger Weishaupt, Johanna Wolfsberger, Irina Alafuzoff, Ann Nordgren, Thierry Magnaldo, Peter Siesjö, John Inge Johnsen, Marcel Kool, Kristiina Tammimies, Anna Darabi, Fredrik J. Swartling, Anna Falk*, and Margareta Wilhelm*

Corresponding authors
Email: margareta.wilhelm@ki.se, anna.falk@ki.se

This PDF file includes:

Other supplementary materials for this manuscript include the following:

www.pnas.org/cgi/doi/10.1073/pnas.1920521117

Material and Methods

Animal models

Female NOD/SCID/IL2Rγ$^{-/-}$ mice aged 8-12 weeks old used for transplantation was purchased from Taconic and housed at approved animal facility at Karolinska Institutet. NES cells (1x10^5 in 2 µl of PBS) were injected using a 30G Hamilton syringe connected to an infusion pump at a rate of 2 µl/10 minutes. Injection coordinates (relative to bregma) are: anterior 6.5 mm, lateral 1.5 mm, 2.5 mm deep. To obtain bioluminescence images, mice were imaged at 1 minute exposure using IVIS SpectrumCT In Vivo Imaging System (PerkinElmer) within 10 minutes after intraperitoneal injection of D-luciferin (BioThema, BT11-1000K) at dosage of 150 mg luciferin/kg body weight. Tumor-bearing mice were sacrificed due to criteria such as visible distress. All animal experiments were conducted in accordance with guidelines of Karolinska Institutet and approved by Stockholm's North Ethical Committee of Animal Research (ethical permits N220/13, 6548/18).

iPSC and NES cell culture

G1 iPS cells reprogrammed from keratinocytes isolated from Gorlin syndrome patient with germline *PTCH1* mutation were generously provided by Professor Austin Smith, University of Cambridge and are described in (1), patient and keratinocytes are described in (2-4); the generation of Control 1 and 3 iPS cells was previously described in (5). iPS cells were cultured in Essential 8™ medium (ThermoFisher Scientific, A1517001) on plates coated with human recombinant Laminin-521 (Biolamina, LN521-03). Enzymatic passaging was performed using TrypLE Select 1X (ThermoFisher Scientific, 12563011) and seeded in media supplemented with 10 µM Y27632 rho-kinase inhibitor or ROCKi (Millipore, SCM075). NES cells were derived as previously described (6, 7). Briefly, iPS cells were incubated with 3 µM glycogen synthase kinase (GSK3) inhibitor (CHIR99021, Tocris #4423)), 2 µM transforming growth factor beta receptor inhibitor (SB-431542, Tocris #1614)), and 2 µM gamma-secretase inhibitor N-(N-(3,5-difluorophenacetyl)-l-alanyl)-S-phenylglycine t-butyl ester (DAPT; Sigma-Aldrich, D5942) for 5 to 7 days when neural rosettes appear and were manually picked. NES cells are grown in high density monolayers (4x10^4/cm^2), passaged using TrypLE™ (ThermoFisher Scientific, 12604054) and plated onto plates coated with 0,1 mg/ml Poly-L-ornithine and 1 µg/ml laminin

(Sigma, P3655-100MG and L2020, respectively) in NES culture media (DMEM/F12+GlutaMax (ThermoFisher Scientific, cat: 31331-028) containing 1x N2 supplement (ThermoFisher, 17504-044), 0.1% B27 supplement (ThermoFisher Scientific, 17502-048), 10 ng/ml FGF2 (LifeTechnologies, PHG0023), 10 ng/ml EGF (PeproTech AF100-15) and Penicillin-streptomycin (ThermoFisher Scientific, 15140-122). NES cells were fed on a daily basis and passaged every third day in 1:3 ratios.

Neuronal Differentiation

Cells were seeded on poly-L-ornithine/laminin-coated 24-well plates in NES media at density $2.6x10^4$ cells/cm^2 (NES) or $1.3x10^4$ cells/cm^2 (tNES). Neuronal differentiation was induced by removing growth factors FGF2 and EGF from the media and culturing the cells in DMEM/F12 media supplemented with 1xN2, 0.1% B27, and 1% Pen/Strep (all from ThermoFisher Scientific).

Cyto- and molecular genetic analyses

For karyotyping, NES cells were seeded on poly-L-ornithine/laminin-coated 6 well plates and then treated with Colcemid for 16-18 hours. Following cell harvesting, metaphase slides were prepared according to standard procedures. Chromosome analysis was performed after GTG-banding with a resolution of approximately 550 bands per haploid genome. Additionally, DNA samples from one of the Gorlin NES, tNES and secondary tNES were used for exome sequencing. In brief, 50 ng of genomic DNA was used for library preparation using the Twist Human Core Exome v1.3 Enrichment Kit (Twist Bioscience) with the minor modifications on the adapters and PCR amplication. Sequencing was done on NovaSeq 6000 using paired-end 150 bp readout. Demultiplexing was done using Casava v2.20. Joint variant calling was performed using GATK standard pipeline.

In vitro viability assay

For evaluation of cell proliferation at different time points, NES cells and tNES cells were seeded on poly-L-ornithine/laminin-coated 24-well tissue culture plates at a density of $2x10^4$ cells/well. The cells were trypsinized and counted on stated days to determine the

number of viable cells. For proliferation in hypoxia, the cells were cultured in hypoxia chamber containing 1% O_2. For treatment of NES and tNES cells, cells were seeded in poly-L-ornithine/laminin-coated 48-well tissue culture plates at $3x10^4$ cells/well and treated with Vismodegib (GDC-0449) (BioVision) or OTX008 (Axon Medchem) for 72 hours with a media change after 36 hours. For treatment of DAOY cells, cells were plated at $2x10^4$ cells/well and treated. Thereafter, cells were incubated with 25 µg/mL Resazurin for 4 hours at 37°C before the absorbance of the supernatant was measured at 560 nm using a microplate reader. For evaluation of cell viability in media with no growth factors, cells grown in normal media were passaged then washed and plated in media with no growth factors.

Cell migration assay

Cells were seeded on poly-L-ornithine/laminin-coated 96-well plates at $6.0x10^4$ cells/well. G1 parental cells were seeded at $1.0x10^5$ cells/well to reach full confluency. After one day, the scratch was performed using Woundmaker (IncuCyte; 4493), the cells were washed with PBS and NES media was changed before migration of the cells was assessed. For this, IncuCyte S3 Live-Cell Analysis System was used to follow wound healing progression every 6 hours for in total 36 hours. Images were analyzed using IncuCyte S3 Software.

Invasion assay

Cells were plated onto poly-L-ornithine/laminin-coated 6-well plates at density of $3x10^5$ cells/well and kept overnight before starvation using NES culture media with 1/10 amount of media supplements for 6 hours. The cells were then detached and washed in media with no growth factors and plated on CultreCoat® 24-well Low BME Cell Invasion Inserts (Trevigen; 3481-024-01) at density of $1.2x10^5$ cells/insert in 120 µl of NES media with 1/10 supplements. The bottom chambers contained NES media with 1x supplements. Cells were incubated for 72 hours before removal of cells from the inserts and the inserts were stained with Cell Stain Solution (CytoSelect™; 11002) for 10 minutes. The amount of cell invasion was quantified by extracting the staining using Extraction Solution (CytoSelect™; 11003) and measuring the absorbance of supernatant at 560nm.

Neurosphere assay

Cells were plated at a density of $5x10^3$ cells/well on 24-well ultra-low attachment plates (Sigma Aldrich; CLS3473-24EA) with 0.5 ml NES medium for 3 days. The number of spheres was counted under microscope and the size of spheres formed was measured using ImageJ software.

Real-time quantitative PCR

For RNA extraction, cells were lyzed using TRIzol® Reagent. Total RNA was isolated using Direct-zol RNA MiniPrep (Zymo Research) kit according to manufacturer's instructions. The complimentary DNA was synthesized using iScript™ cDNA (BioRad) and real-time PCR (iTaq universal SYBR Green Supermix, BioRad) was performed using ABI StepOne machine. Each PCR experiment was carried out in triplicate for each gene. Fold changes in the genes of interest were calculated after normalization with endogenous controls (β-actin, 28s, GAPDH or α-Tubulin) and using the comparative threshold (ΔΔCt) method. The primer sequences are listed in Supplementary Table S1.

Western blot analysis.

For PTCH1 protein detection, cells were lyzed in buffer containing 10 mM Tris-HCl pH8, 140 mM NaCl, 300 mM KCl, 1 mM EDTA, 0.5% Triton X-100, 0.5% Sodium deoxycholate, + Complete protease inhibitor cocktail (Roche). For Galectin-1 and Gli-1 detection, cells were lyzed in RIPA buffer (Sigma) with 1x Halt™ Protease and Phosphatase Inhibitor Cocktail (Thermo Fisher Scientific). Final protein concentration of the cell lysates was determined using the bicinchoninic acid (BCA) method with bovine serum albumin (BSA) as the standard. Equal amounts of total protein extracts were separated by SDS-PAGE (Bolt™ 3-8% Tris-Acetate gel or 12% Tris-Bis gel,) and electro-transferred to polyvinylidene fluoride membranes or nitrocellulose membrane (BioRad). Primary antibodies (listed in Supplementary Table S2) were diluted in TBST (TBST/tween; 5% milk powder or 5% BSA) and incubated with the membranes at 4°C overnight. The appropriate secondary antibody conjugated to horseradish peroxidase was applied at room temperature for 1 hour. Immunoreactive proteins were developed using

ECL Plus western blotting detection kit (GE Healthcare) or ECL SuperSignal West Dura Extended Duration Substrate kit (Thermo Fisher Scientific).

Immunohistochemistry

Paraffin-embedded tumor tissue were dewaxed, rehydrated, and stained with hematoxylin and eosin (Histolab and Sigma-Aldrich, respectively) or immunostained. For immunohistochemistry, citrate buffer (pH 6) was used in antigen retrieval process. Endogenous peroxidases were blocked with 3% hydrogen peroxide (Sigma-Aldich). Tissues were blocked using normal goat serum and incubated with primary antibodies overnight at 4°C followed by biotinylated secondary antibodies (Vector Laboratories) for one hour, and Vectastain Elite (avidin-HRP; Vector Laboratories) for 30 minutes. Then, samples were developed with diaminobenzidine chromogen (Vector Laboratories), counterstained with Hematoxylin and mounted with a cover slip containing DPX mountant. Tumors from at least three different mice were analyzed for each staining. Human-specific nuclei staining was performed on OCT-frozen tumors. The collection and analysis of human medulloblastoma samples in the study was approved by The Local Ethical Board of Lund University (LU1028-03, ETIK642/2008). MB subgroup affiliation has been described elsewhere (8). Cryosections (6 µm) of human MB samples were thawed for 5 minutes, then acetone-fixed for 10 minutes. Sections were blocked with 5% normal goat serum (Fisher Scientific) for 20 minutes, followed by primary antibody incubation for 60 minutes and secondary antibodies conjugated to Alexa fluorophores (5 µg/ml, Molecular Probes) for 30 minutes. Finally, sections were mounted with ProLong Gold anti fade containing DAPI (Molecular Probes) as nuclear staining. Primary antibodies and dilution are listed in Supplementary table S2.

Immunofluorescence

Cells were fixed in 4% paraformaldehyde for 10 minutes and blocked using 10% FBS and 0.1% Triton in PBS and incubated at room temperature for 1 hour. Cells were incubated with primary antibodies at 4°C overnight. Secondary antibodies conjugated to Alexa fluorophores (1:500, Life Technologies) and incubated for 1 hour at room temperature. Nuclear staining was performed using DAPI (1:5000) and incubated at room temperature

for 10 minutes. Mounting was performed using Fluorescent Mounting medium (Agilent technologies; S302380-2). Primary antibodies and dilution are listed in Supplementary table S2.

Flow Cytometry

For cell cycle analysis, NES cells were detached from the plates with trypLE Express and washed 3 times with PBS and stained using Click-iT EdU Alexa Fluor 647/488 Flow Cytometry Assay Kits (ThermoFisher Scientific; C10420/C10632) according to the manufacturer's instructions. For CD133 staining, cells were resuspended in PBS, and incubated with APC-conjugated mouse anti-human CD133/2 (Miltenyi Biotec) or APC-conjugated isotype control mouse IgG_{2b} (1:10) at 4 °C for 30 minutes in the dark. For Annexin V staining, washed and resuspended cells were stained with PE Annexin V antibody (BD Pharmingen™; 556422) according the manufacturer's instructions. After washing, the labeled cells were analyzed using FACS Calibur flow cytometer (BD Biosciences).

Cell isolation from tumors

A piece of cerebellum was incubated in digestion buffer (1x PBS with 10 U/ml papain, 200 µg/ml L-cysteine, 250 U/ml DNAse, Pen/Strep, all from Sigma Aldrich) at 37ºC for 30 minutes. The cells were centrifuged at room temperature and the buffer was replaced with PBS containing 2 mg/ml soybean trypsin inhibitor (ThermoFisher), 8 mg/ml BSA, 250 U/ml DNAse, Pen/Strep (all from Sigma Aldrich). The cells were triturated using 18G to 22G needles to obtain single-cell suspension, then centrifuged at room temperature, resuspended in PBS with 200 µg/ml BSA and passed through 100 µm cell strainer, centrifuged and resuspended in NES media and plated on poly-L-ornithine/laminin-coated plates. Cells were purified from mouse cell contaminations using Mouse Cell Depletion Kit (Miltenyi Biotec;130-104-694) according to the manufacturer's instructions.

Chromatin Immunoprecipitation Assay

Hyperconfluent DAOY cells were pre-starved for 24 hours in serum-reduced medium, containing 0.5% (v/v) FBS, before treated with 100 nM Smoothened Agonist (SAG) (Sigma-Aldrich, #56661) for 24hours. Cells were cross-linked with 1% formaldehyde, 10 minutes at room temperature, then quenched with 0.125M glycine, before washing and collection in ice cold PBS. Cells were lysed for 10 minutes on ice in ChIP lysis buffer (50 mM Tris (pH 8.0, 140 mM NaCl, 1 mM EDTA, 10% glycerol, 0.5% NP-40, 0.25% Triton X-100, 1× protease inhibitor cocktail), followed by 15 cycles of sonication (30sec pulse/30sec; Amplitude strength 50%, Misonix S-4000 Sonicator system). Immunoprecipitation was performed with 50µg of chromatin overnight at 4°C with 2.5µg antibody per IP (Antibodies listed in Supplementary table S2). Immuno-complexes were captured by Dynabeads Protein G for 2 hours at 4°C, and washed sequentially with Low-salt buffer (20mM Tris-HCl, pH 7.5, 2mM EDTA, 150mM NaCl, 0.5% Triton X-100), High-salt buffer (20mM Tris-HCl, pH 7.5, 2mM EDTA, 500mM NaCl, 0.5% Triton X-100) and washed twice with LiCl buffer (10mM Tris-HCl, pH 7.5, 1mM EDTA, 250mM LiCl, 0.5% Triton X-100, 0.1% SDS) and No-salt buffer (10mM Tris-HCl pH7.5, 1mM EDTA). The immune complex was dissociated from the beads at room temperature for 15 minutes with gentle agitation in ChIP Elution buffer (1% SDS, 0.1M $NaHCO_3$). The reverse crosslinking was performed at 4 hours at 65°C with 0.3M NaCl, followed by a Proteinase K (0.5µg/µl) treatment at 55°C for 1 hour. DNA fragments were purified using the Zymo ChIP DNA Clean & Concentrator kit. Quantitative RT-PCR was performed using 25ng of DNA with primer pairs spanning the predicted binding regions in *LGALS1* promoter.

Lentiviral shRNA-mediated knockdown of *LGALS1*

For preparation of lentiviral particles, pLKO.1-shLGALS1 (Dharmacon, RHS4533-EG3956) or pLKO.1-shCtrl, were co-transfected with pCMV-delta-R8.2 and pCMV-VSV-G into subconfluent HEK293T cells using Lipofectamine 2000 according to manufacturer's instruction (Thermo Fisher Scientific). The cell media was changed to NES media after 6 hours incubation and supernatant containing lentiviral particles were harvested 48 hours later. Secondary tNES cells were pelleted and resuspended in complete

NES media containing lentiviral supernatant (1:5), incubated for 10 minutes at room temperature and plated at a density of 120,000 cells/well on poly-L-ornithine/laminin-coated 24-well plates. 48 hours after viral transduction, when cells were confluent, a scratch was made manually, and media was changed to NES media containing Laminin (1:1000). Cells were imaged at 0, 24, 48 hours and images were analyzed using ImageJ. *LGALS1* gene expression was examined using qRT-PCR 48 hours after transduction.

Quantification and Statistical Analyses

All values are expressed as Mean ± SD as indicated. Statistical analyses were performed with the Student *t* test, one-way or two-way ANOVA with Tukey, or Dunnett. P-values <0.05 were considered statistically significant. All data analyses were performed using GraphPad Prism 6. $^{*}P < 0.05$, $^{**}P < 0.01$, $^{***}P < 0.001$, $^{****}P < 0.0001$.

RNA sequencing

For RNA extraction, NES and tNES monolayer cells were lyzed using TRIzol® Reagent. Total RNA was isolated using Direct-zol RNA MiniPrep (Zymo Research) kit according to manufacturer's instructions. RNA-Seq was performed at Uppsala Genome Center, SciLifeLab, Uppsala University on Ion-Proton platform using IonXpress. All RNA sequence reads were mapped against the human genome assembly GRCh37/hg19 using STAR v2.4.0 (9). The alignment was performed with a two-pass approach where splice junctions discovered during a first alignment guides the forming of a final second alignment (10). Unmapped reads were realigned using Bowtie2 v2.2.3 (11) before duplicate reads were removed with Picard v1.127. The transcriptome was then assembled, and its expression profile quantified with Cufflinks v2.2.1 (12).

Gene set enrichment analysis

Gene Set Enrichment Analysis (13) (GSEA) was performed using GSEA v.2.2.3 software downloaded from Broad institute (http://software.broadinstitute.org/ gsea/). The gene expression dataset was processed with the R package plyr (14), by which multiple probes corresponding to a single gene were merged using average expression value. The dataset

was then analyzed against the Gene Ontology (GO), Reactome, Panther, NetPath, HumanCyc, NCI Pathway Interaction Database (PID), MSigDB Hallmark and the MSigDB KEGG and Oncogenic gene set collections downloaded from http://baderlab.org/GeneSets on 1 February 2019 according to the Reimand protocol (15) The enriched pathways were visualized by Cytoscape EnrichmentMap and AutoAnnotate application (15, 16).

Analysis of the correlation between the expression of genes of interest with human patient data

Gene expression data of human MB samples come from public sources deposited in GEO (http://www.ncbi.nlm.nih.gov/geo) or available at R2 (http://R2.amc.nl) (GSE85218 (17), GSE37385 (18), GSE10327 (19), GSE37418 (20), GSE12992 (21), GSE3526 (22), GSE35493 (23), and (24)). The MAS5.0 algorithm of the GCOS program (Affymetrix Inc) was used for normalization of the expression data. All data have been analyzed using the R2 program for analysis and visualization of microarray data (http://R2.amc.nl). Anova tests were used to test whether there is a significant differential expression between the groups shown in the plots.

Principal component analysis

Gene expression datasets used for reference were downloaded from Gene Expression Omnibus (GSE25219, GSE50161, GSE37418, GSE85218) (17, 20, 25, 26). The reference data were downloaded as raw CEL files and preprocessed using the R package oligo (27) and hgu133plus2.db (28). Principal component analysis based on metagenes were performed using the Metagene code for cross-platform, cross-species characterization of global transcriptional states (29).

Differential gene expression analysis

Differential gene expression was performed using the R-package CummeRbund (30). FPKM values were adjusted to FPKM + 1 in order to include genes with zero expression in fold change calculation.

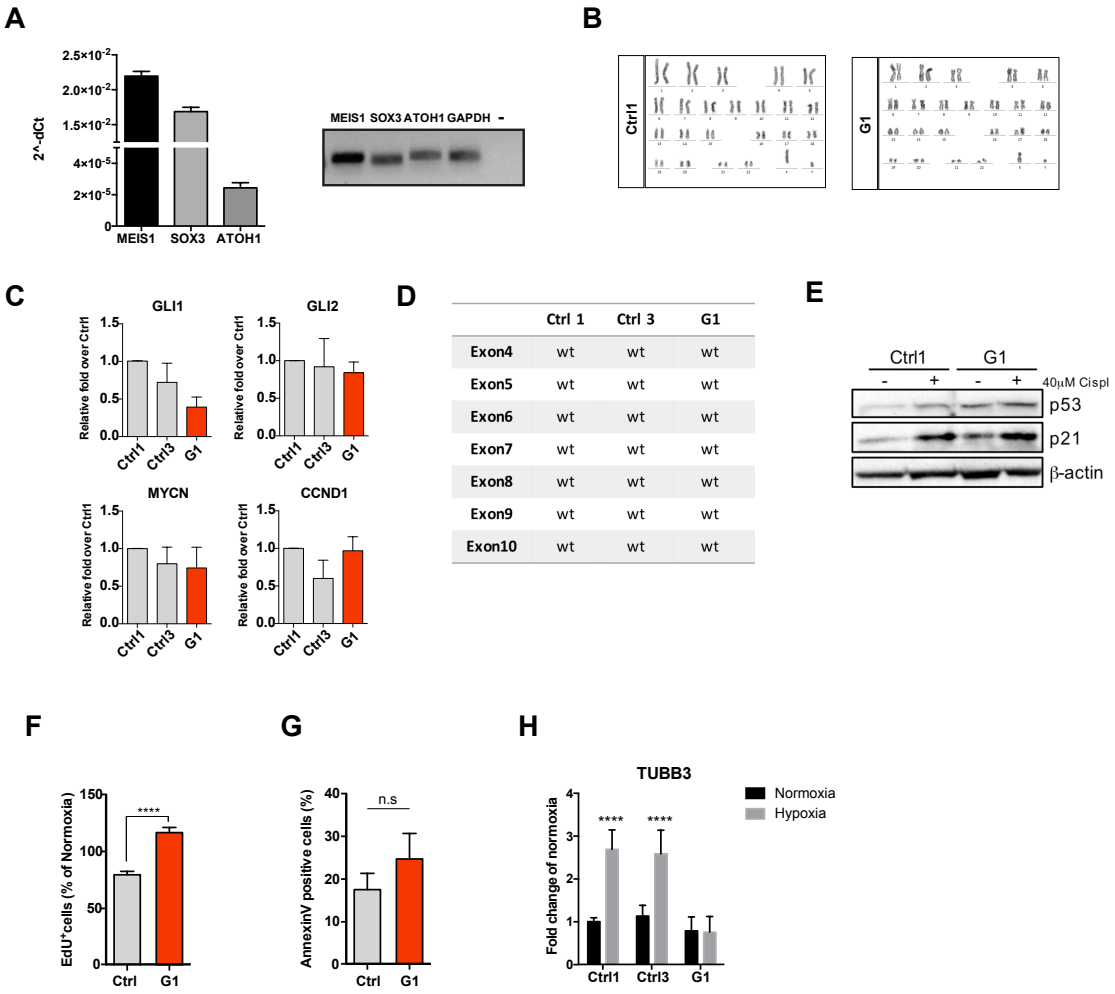

Supplementary Figure S1 related to Figure 1. (A) Expression of EGL and neural stem cell markers, left panel: qRT-PCR showing normalized mRNA expression presented as 2^{-dCT}, data presented as Mean± SD. right panel, PCR products from semi-quantitative RT-PCR. (B) The NES cells were karyotypically normal. Chromosome analysis was performed after GTG-banding with a resolution of approximately 550 bands per haploid genome. (C) qRT-PCR analysis of SHH target gene expression in Gorlin and Control NES cells. Data is shown as Mean ± SD, representing three independent experiments. (D) Results of sequencing of exons 4 to 9 of *TP53* gene in Ctrl1, Ctrl3, and G1 NES cells. (E) Western blot analysis of Ctrl1, and G1 NES cells treated for 16h with 40μM Cisplatin showed upregulation of p53 protein as well as p21, indicating functional p53 protein. (F) ClickIT EdU Flow cytometry data is expressed as fold over cell number in normoxia. Mean ± SD, n=3, ****P≤0.0001, student t-test. (G) Annexin V/PI Flow cytometry analysis of G1 and Control NES cells in hypoxia, expressed as percentage of AnnexinV positive cells out of live cells. Mean ± SD, n=3 independent experiments, n.s= not significant student t-test. (H) Analysis of *TUBB3* expression in cells grown in hypoxia (1% O_2, 96hrs) using qRT-PCR. Data are presented as relative fold change compared to normoxia and shown as Mean ± SD, n=3 ****P≤0.0001 *t-test*.

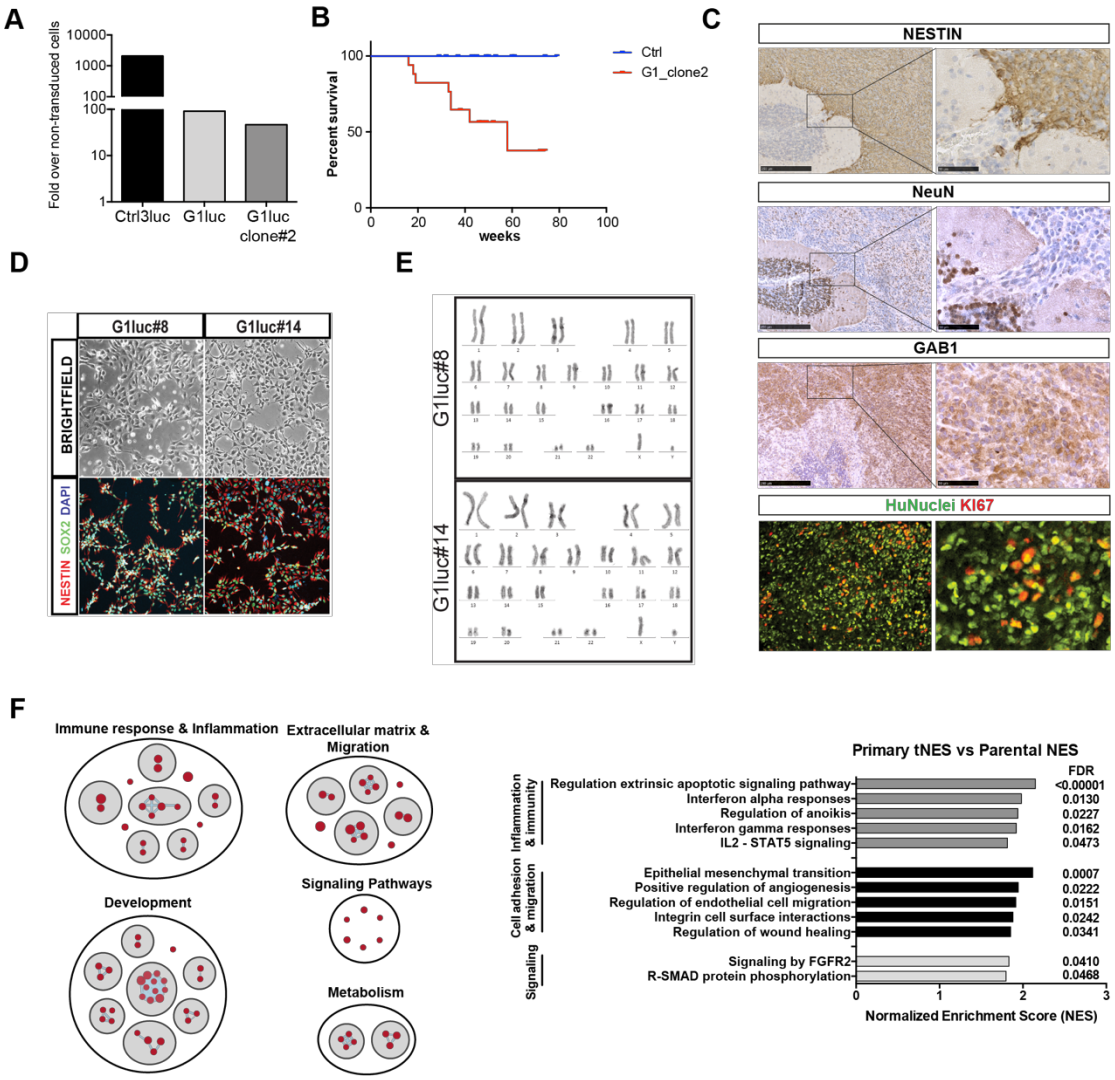

Supplementary Figure S2 related to Figure 2 (A) Activity of luciferase gene reporter in Ctrl3luc, G1luc, and G1luc clone#2 NES cells as measured by luciferase substrate addition and luminescence reading. (B) Overall survival analysis of NSG mice injected with Ctrl n=14 or G1luc clone #2 (n=19). Kaplan-Meier curves depict differences in survival and statistical differences determined using the log rank test. G1luc clone#2 P=0.0046. (C) Cerebellar tumor sections were stained for NESTIN, GAB1 and NeuN. Tumors were positive for human nuclei (HuNuclei, green) showing human origin, some of which were proliferating cells (KI67 red), Left panel bar 250 µm, Right panel bar 50 µm. (D) Examples of tumor-isolated (tNES) cells from different primary tumors (G1luc#8 and G1Aluc#14), expressing NESTIN and SOX2, bar 100 µm. (E) The tNES cells had normal karyotype, indicating no gross chromosomal changes during in vivo growth. (F) Left panel: Enrichment map generated by Broad Institute GSEA tool (FDR<0.05) and visualized by Cytoscape EnrichmentMap and AutoAnnotate application, showing biological pathways enriched in G1 primary tNES cells compared to parental NES cells. Red nodes represent upregulated biological pathways, blue lines represent gene overlap between pathways. Right Panel: Histogram of most significantly deregulated pathways in G1 primary tNES compared to Parental G1 NES.

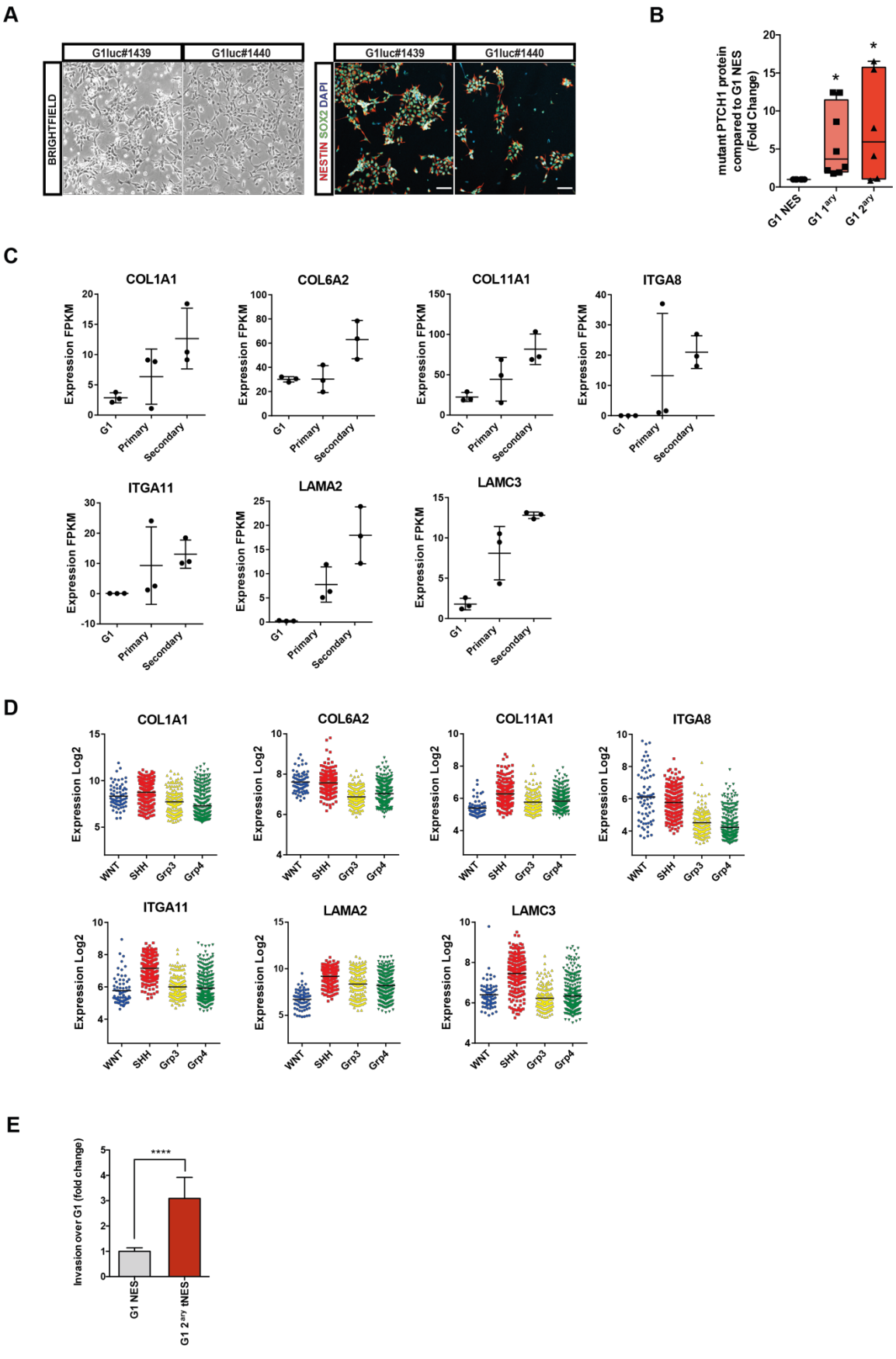
A
G1luc#1439
G1luc#1440
BRIGHTFIELD
NESTIN SOX2 DAPI
B
mutant PTCH1 protein compared to G1 NES (Fold Change)
G1 NES
G1 1ary
G1 2ary
C
COL1A1
COL6A2
COL11A1
ITGA8
ITGA11
LAMA2
LAMC3
Expression FPKM
G1
Primary
Secondary
D
Expression Log2
WNT
SHH
Grp3
Grp4
E
Invasion over G1 (fold change)
****
G1 NES
G1 2ary tNES

Supplementary Figure S3 related to Figure 3 and 5 (A) Representative examples of secondary tumor-derived cells isolated from orthotopic injection of G1luc#14 tNES (tumors G1luc#1439 and G1luc#1440). Secondary tNES cells could be cultured for many passages and they express the stem cell markers NESTIN and SOX2, bar 100µm. (B) Quantification of western blot analysis of mutant PTCH1 protein in G1 NES (n=6), primary tNES (n=8), and secondary tNES (n=6) *P≤0.05, unpaired *t* test (C) RNA sequencing results indicated an increase in the gene expression of Collagens *COL1A1*, *COL6A2*, *COL11A1*, Integrins *ITGA8*, *ITGA11*, and Laminins *LAMA2*, *LAMC3* in G1 primary and secondary tumor cells compared to G1 parental cells. (D) These genes were also highly expressed in published datasets of human SHH medulloblastoma samples (39). (E) G1 secondary tNES cells have higher invasion ability compared to parental cells in transwell invasion assay. Mean ± SD, n=3, ****P≤0.0001, unpaired *t* test.

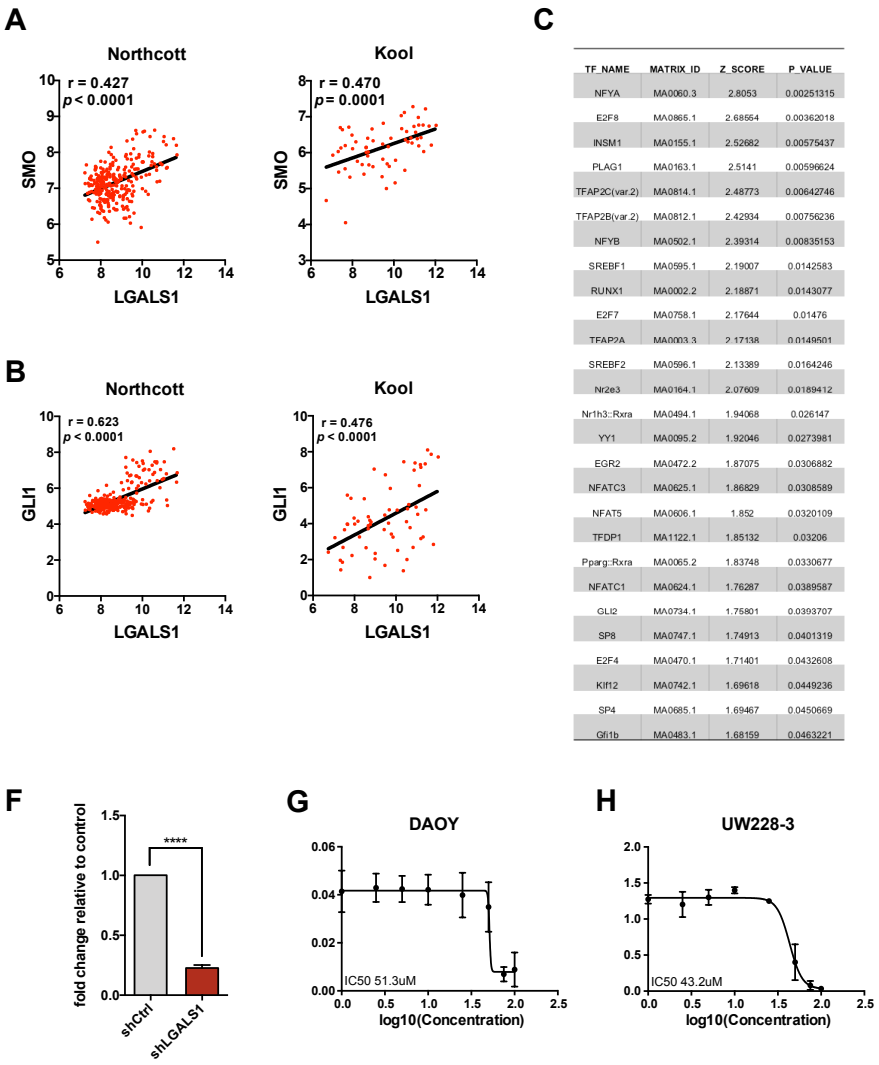

Supplementary Figure S4 related to Figure 6. (A and B). The expression of *LGALS1* correlated to the expression of *SMO* and *GLI1* genes in Northcott (GSE37382) and Kool (GSE10327) public datasets. (C) Analysis of transcription factor binding sites in the human *LGALS1* promoter using the Pscan tool. (D) GLI2 ChIP of DAOY cells treated with SAG and qPCR analysis using primers flanking GLI-bindings site in *LGALS1* promoter. Mean ± SD, n=3, **P≤0.01 student t-test. (E) H3K9ac ChIP of DAOY cells treated with SAG and qPCR analysis using primers flanking GLI-bindings site in *LGALS1* promoter. Mean ± SD, n=3, ****P≤0.0001 student t-test. (F) qRT-PCR analysis of *LGALS1* expression in secondary tNES cells transduced with control shRNA or shRNA targeting *LGALS1*. Data is shown as Mean ± SD, representing three independent experiments. ****P≤0.0001 student t-test (G) Treatment of DAOY cells with increasing concentration of OTX008 for 72hrs and measuring viability using crystal violet assay. IC50~51.3µM. (H) Treatment of UW228-3 cells with increasing concentration of OTX008 for 72hrs and measuring viability using crystal violet assay. IC50~43.2µM.

Table S1. **Oligonucleotides**

TP53 exon 4 forward	5′-GGACTGACTTTCTGCTCTTGTCTTT-3′
TP53 exon 4 reverse	5′-CAGAGATCACACATTAAGTGGGTAA-3′
TP53 exon 5 forward	5′-CTCTCTAGCTCGCTAGTGGGT-3′
TP53 exon 5 reverse	5′-CGAAAAGTGTTTCTGTCATCCAAAT-3′
TP53 exon 6 forward	5′-GCCATGGCCATCTACAAGCA-3′
TP53 exon 6 reverse	5′-TGGGGTTATAGGGAGGTCAAA-3′
TP53 exon 7 forward	5′-ACAGGTCTCCCCAAGG-3′
TP53 exon 7 reverse	5′-AAACTGAGTGGGAGCAGTAAGGAGA-3′
TP53 exon 8 + 9 forward	5′- GGACAAGGGTGGTTGGGAGTAGA-3′
TP53 exon 8 + 9 reverse	5′-CCCAATTGCAGGTAAAACAGTCAAG-3′
TP53 exon 10 forward	5′-CAGTTTCTACTAAATGCATGTTGCT-3′
TP53 exon 10 reverse	5′-ATACACTGAGGCAAGAATGTGGTTA-3′
TP53 exon 11 forward	5′-CATCTTGATTTGAATTCCCGTTGT-3′
TP53 exon 11 reverse	5′-CACCAGTGCAGGCCAACTTGTTCAG-3′
PTCH1 exon 13 forward	5´-TTAAAACCTCAGGGGACACG-3´
PTCH1 exon 13 reverse	5´-GAAGCAGCCTCTGTCCAATC-3´
LGALS1 forward	5′-TCGCCAGCAACCTGAATCTC-3′
LGALS1 reverse	5′-GCACGAAGCTCTTAGCGTCA-3′
HHIP forward	5´-TCTCAAAGCCTGTTCCACTCA-3´
HHIP reverse	5´-GCCTCGGCAAGTGTAAAAGAA-3´
α-tubulin forward	5′-ACCTTAACCGCCTTATTAGCCA-3′
α-tubulin reverse	5′-ACATTCAGGGCTCCATCAAATC-3′
28s forward	5´-TTGAAAATCCGGGGGAGAG-3´
28s reverse	5´-ACATTGTTCCAACATGCCAG-3´
β-actin forward	5´-CATGTACGTTGCTATCCAGGC-3´
β-actin reverse	5´-CTCCTTAATGTCACGCACGAT-3´
GLI1 forward	5´-CAGCTACATCAACTCCGGCCAATAGGG-3´
GLI1 reverse	5´-TGCTGCGGCGTTCAAGAGAGACTG-3´
SNAI2 forward	5´-CGAACTGGACACACATACAGTG-3´
SNAI2 reverse	5´-CTGAGGATCTCTGGTTGTGGT-3´
CCND1 forward	5′-ACGAAGGTCTGCGCGTGTT-3′

CCND1 reverse	5’-CCGCTGGCCATGAACTACCT-3’
GLI2 forward	5’-CGAGAAACCCTACATCTGCAAGA-3’
GLI2 reverse	5’-TTTCACATGCTTCCGGAGAGA-3’
NMYC forward	5’-CCGGGCATGATCTGCAA-3’
NMYC reverse	5’-CCGCCGAAGTAGAAGTCATCTT-3’
TUBB3 forward	5´-GGCCAAGGGTCACTACACG-3´
TUBB3 reverse	5´-GCAGTCGCAGTTTTCACACTC-3´
LGALS1 promoter forward	5’-TGCTGAACA CTCAGGGAAGG-3’
LGALS1 promoter reverse	5’-CTCTCGGGTGGAGTCTTCTG-3’
MEIS1 forward	5’-GGGCATGGATGGAGTAGG-3’
MEIS1 reverse	5’-GGGTACTGATGCGAGTGCAG-3’
SOX3 forward	5’-GACCTGTTCGAGAGAACTCATCA-3’
SOX3 reverse	5’-CGGGAAGGGTAGGCTTATCAA-3’
ATOH1 forward	5´-CCTTCCAGCAAACAGGTGAAT-3´
ATOH1 reverse	5´-TTGTTGAACGACGGGATAACAT-3´

Table S2. **Antibodies**

Antibody target	Source	Identifier	Dilution
Ki-67	abcam	ab15580	1:200
Tuj1	abcam	ab7751	1:200
Nestin	Millipore	MAB5326-KC	1:200
NeuN	Millipore	ABN78	1:500
Synapthophysin	abcam	ab32127	1:200
human nuclei	Merck	MAB1281	1:500
Galectin-1 (IHC)	abcam	ab25138	1:1000
Galectin-1(8A12) (WB)	Cell Signaling	40103	1:500
CD45	BD Pharmingen	555483	1:10
CD31	abcam	ab9498	1:20
Sox2	Millipore	AB5603	1:500
p53	Santa Cruz Biotech	sc126	1:1000
p21	Santa Cruz Biotech	sc53870	1:200
β-actin	abcam	ab8227	1:1000
GAB1	Cell Signaling	#3232	1:50
DCX	Cell Signaling	#4604	1:1000
PLZF	Invitrogen	#PA5-29213	1:1000
ZO-1	Life Technologies	40-2200	1:1000
Cleaved Caspase 3	Cell Signaling	#9661	1:1000
PTCH1	abcam	53715	1:1000
GLI1	Cell Signaling	#2553	1:500
GLI1	Novus Biological	NB600-600	2.5μg (ChIP)
GLI2	acbam	ab26056	2.5μg (ChIP)
H3K9Ac	Novus Biological	NB21-1074	2.5μg (ChIP)
IgG Isotype control	Novus Biologicals	NBP2-2489	2.5μg (ChIP)
α-Tubulin	Santa Cruz Biotech		1:2000

.

Dataset S1. List of significant gene expression changes in G1 primary tNES cells compared to parental NES. Related to Figure 2 and Figure S2

Dataset S2. Gene set enrichment analysis of G1 primary tNES cells compared to parental NES. Related to Figure S2.

Dataset S3. List of significant gene expression changes in G1 secondary tNES cells compared to G1 primary tNES cells. Related to Figure 5

Dataset S4. Gene set enrichment analysis of G1 secondary tNES cells compared to G1 primary tNES cells. Related to Figure 5

SI References

1. Huang M, *et al.* (2019) Engineering Genetic Predisposition in Human Neuroepithelial Stem Cells Recapitulates Medulloblastoma Tumorigenesis. *Cell Stem Cell*.
2. Brellier F, *et al.* (2008) Ultraviolet responses of Gorlin syndrome primary skin cells. *Br J Dermatol* 159(2):445-452.
3. Valin A, *et al.* (2009) PTCH1 +/- dermal fibroblasts isolated from healthy skin of Gorlin syndrome patients exhibit features of carcinoma associated fibroblasts. *PLoS One* 4(3):e4818.
4. Wright AT, *et al.* (2015) Deficient expression of aldehyde dehydrogenase 1A1 is consistent with increased sensitivity of Gorlin syndrome patients to radiation carcinogenesis. *Mol Carcinog* 54(6):473-484.
5. Wu S, *et al.* (2014) Spider silk for xeno-free long-term self-renewal and differentiation of human pluripotent stem cells. *Biomaterials* 35(30):8496-8502.
6. Falk A, *et al.* (2012) Capture of neuroepithelial-like stem cells from pluripotent stem cells provides a versatile system for in vitro production of human neurons. *PLoS One* 7(1):e29597.
7. Shahsavani M, *et al.* (2017) An in vitro model of lissencephaly: expanding the role of DCX during neurogenesis. *Molecular psychiatry*.
8. Sanden E, *et al.* (2015) Aberrant immunostaining pattern of the CD24 glycoprotein in clinical samples and experimental models of pediatric medulloblastomas. *J Neurooncol* 123(1):1-13.
9. Dobin A, *et al.* (2013) STAR: ultrafast universal RNA-seq aligner. *Bioinformatics* 29(1):15-21.
10. Veeneman BA, Shukla S, Dhanasekaran SM, Chinnaiyan AM, & Nesvizhskii AI (2016) Two-pass alignment improves novel splice junction quantification. *Bioinformatics* 32(1):43-49.
11. Langmead B & Salzberg SL (2012) Fast gapped-read alignment with Bowtie 2. *Nature methods* 9(4):357-359.

12. Trapnell C*, et al.* (2010) Transcript assembly and quantification by RNA-Seq reveals unannotated transcripts and isoform switching during cell differentiation. *Nature biotechnology* 28(5):511-515.
13. Subramanian A*, et al.* (2005) Gene set enrichment analysis: a knowledge-based approach for interpreting genome-wide expression profiles. *Proceedings of the National Academy of Sciences of the United States of America* 102(43):15545-15550.
14. Wickham H (2011) The Split-Apply-Combine Strategy for Data Analysis. *Journal of Statistical Software* 40(1):1-29.
15. Reimand J*, et al.* (2019) Pathway enrichment analysis and visualization of omics data using g:Profiler, GSEA, Cytoscape and EnrichmentMap. *Nat Protoc* 14(2):482-517.
16. Shannon P*, et al.* (2003) Cytoscape: a software environment for integrated models of biomolecular interaction networks. *Genome Res* 13(11):2498-2504.
17. Cavalli FMG*, et al.* (2017) Intertumoral Heterogeneity within Medulloblastoma Subgroups. *Cancer Cell* 31(6):737-754 e736.
18. Northcott PA*, et al.* (2012) Subgroup-specific structural variation across 1,000 medulloblastoma genomes. *Nature* 488(7409):49-56.
19. Kool M*, et al.* (2008) Integrated genomics identifies five medulloblastoma subtypes with distinct genetic profiles, pathway signatures and clinicopathological features. *PloS one* 3(8):e3088.
20. Robinson G*, et al.* (2012) Novel mutations target distinct subgroups of medulloblastoma. *Nature* 488(7409):43-48.
21. Fattet S*, et al.* (2009) Beta-catenin status in paediatric medulloblastomas: correlation of immunohistochemical expression with mutational status, genetic profiles, and clinical characteristics. *J Pathol* 218(1):86-94.
22. Roth RB*, et al.* (2006) Gene expression analyses reveal molecular relationships among 20 regions of the human CNS. *Neurogenetics* 7(2):67-80.
23. Birks DK*, et al.* (2013) Pediatric rhabdoid tumors of kidney and brain show many differences in gene expression but share dysregulation of cell cycle and epigenetic effector genes. *Pediatric blood & cancer* 60(7):1095-1102.
24. Northcott PA*, et al.* (2017) The whole-genome landscape of medulloblastoma subtypes. *Nature* 547(7663):311-317.
25. Kang HJ*, et al.* (2011) Spatio-temporal transcriptome of the human brain. *Nature* 478(7370):483-489.
26. Griesinger AM*, et al.* (2013) Characterization of distinct immunophenotypes across pediatric brain tumor types. *J Immunol* 191(9):4880-4888.
27. Carvalho BS & Irizarry RA (2010) A framework for oligonucleotide microarray preprocessing. *Bioinformatics* 26(19):2363-2367.
28. Carlson M (2016) hgu133plus2.db: Affymetrix Human Genome U133 Plus 2.0 Array annotation data (chip hgu133plus2).
29. Tamayo P SD, Ebert B.L, Gillette M.A, Roberts C.W.M, Mesirow J.P (2007) Metagene projection for cross-platform, cross-species characterization of global transcriptional states. *PNAS*.

30. Trapnell C*, et al.* (2012) Differential gene and transcript expression analysis of RNA-seq experiments with TopHat and Cufflinks. *Nature protocols* 7(3):562-578.